# RSC Advances

## RSC Advances

www.rsc.org/advances

ROYAL SOCIETY OF CHEMISTRY

www.rsc.org/advances

# Phase Behaviors of Side Chain Liquid Crystalline Block Copolymers

*Xiaokang Li,[a] Feng Huang,[a] Tao Jiang,[a] Xiaohua He,[b] Shaoliang Lin,[*,a] and Jiaping Lin[*,a]*

*[a] Shanghai Key Laboratory of Advanced Polymeric Materials, Key Laboratory for Ultrafine Materials of Ministry of Education, School of Materials Science and Engineering, East China University of Science and Technology, Shanghai 200237, China*

*[b] Department of Chemistry, East China Normal University, Shanghai 200241, China*

[*] Tel: +86-21-6425-1011

E-mail: slin@ecust.edu.cn (S.L.); jlin@ecust.edu.cn (J.L.)

**ABSTRACT:** Microphase separation of side chain liquid crystalline (SCLC) block copolymers were studied by dissipative particle dynamics (DPD) simulations. The block copolymer monomer consists of flexible **A** segments and flexible **B** segments grafted by rigid **C** side chains, where the **A**, **B** and **C** blocks are incompatible with each other. The phase structures of SCLC copolymers were found to be controlled by **A**, **C** block lengths and graft number. Various mesophases, such as sphere, cylinder, gyroid, and lamella were obtained. Phase stability regions in space of **C** block length and **A** block length (or graft number and **A** block length) were constructed. The packing ordering of **C** side chains was also studied, and discovered to increase as the temperature decreases or the rigid **C** side chains increase. In addition, the results of SCLC copolymers were compared with flexible copolymers and available experimental observations. The simulation results in the present work provide useful information for future investigations on SCLC copolymers.

## 1.  INTRODUCTION

In recent decades, the phase behaviors of block copolymers have attracted much attention due to their promising applications in coating and adhesive films.[1-6] The block copolymers can form classical microstructures including lamella, bicontinuous gyroid, hexagonally packed cylinders, and body-centered cubic spheres, as a consequence of microphase separation between different blocks.[7-11] So far most block copolymers studied are flexible copolymers. In contrast with flexible block copolymers, block copolymers containing rigid segments (liquid crystalline copolymers) can form nanostructures with higher ordering degree, since the rigid segments can lead to orientation organization.[12-16] When the rigid segments act as side chains to be grafted on a polymer backbone, a side chain liquid crystalline (SCLC) block copolymer is obtained. The SCLC copolymers possess both characteristics of graft copolymer and liquid crystalline copolymer, which may provide potential applications in fields of biomedicine and nanotechnology.[17-21]

Experimentally, the SCLC block copolymers have been widely applied to prepare a variety of ordered nanostructures.[22-33] The phase behaviors of SCLC block copolymers are much complicated due to the coexistence of microphase separation and orientation packing of rigid segments.[26-34] de Wit and coworkers reported the phase behavior of poly(4-vinylpyridine) (P4VP)-based azobenzene-containing copolymers as investigated by DSC and simultaneous SAXS/WAXS.[26] They found that the SCLC copolymers tend to form lamellar phase and exhibit smectic ordering in the azobenzene domain. Korhonen *et al*. synthesized a series of SCLC block copolymers through attaching rigid cholesteryl hemisuccinate (CholHS) to flexible poly(styrene)-*b*-poly(4-vinylpyridine) (PS-*b*-P4VP) block copolymers.[34] The SCLC copolymers can self-assemble into hierarchical structures in which the smectic layers of CholHS are perpendicular to the block domain interface. However, due to the structural complexities of SCLC copolymers and the limitations of experimental technology, many

important issues, including the chain packing and influencing mechanism of external factors on the phase behavior, are little understood.

Apart from the experimental observations, theories and computer simulations have emerged as powerful tools to study the phase behaviors of complex polymers.[35-43] They can provide more straightforward results than pure experiments, and overcome the limitation inherent in experiments. So far, various approaches, such as self-consistent field theory (SCFT),[35,36] Monte Carlo (MC) simulations,[37] molecular dynamics (MD) simulations,[38] and dissipative particle dynamics (DPD) simulations,[39,40] have been widely employed to investigate the phase behaviors of flexible block and graft copolymers. However, theoretical and simulation studies on the phase behavior of SCLC block copolymers are very limited.[41-43] For example, Shah and coworkers proposed a SCFT model and a strong segregation theory (SST) based analytical theory to understand the thermodynamic behavior of SCLC block copolymers.[41] The SCLC copolymer can phase separate into lamellar and cylindrical phases with rigid blocks in dispersed or continuous domains. In the lamellae, the orientation direction of rigid side chains is parallel to the block copolymers interface, while in the cylinders it is parallel to the long axis of cylinders. Stimson *et al*. carried out MD simulations on the phase structures of polysiloxane SCLC block copolymers.[43] The SCLC copolymers self-organize into lamellar phases with polymeric-rich and mesogenic-rich regions as the systems are cooled from fully isotropic polymer melts. Within the smectic phases, the backbone was perpendicular to the directors of smectic-A. Compared with SCFT and MD simulations, DPD simulation can access larger length and time scales, and thus presents more predominant in the study of the phase behaviors of polymers. However, to the best of our knowledge, no studies of phase behavior of SCLC block copolymers using the DPD method have been reported. Many issues remain to be solved in the complex system, and microphase separation of the SCLC block copolymers need to be explored further.

Understanding the principles of phase separation and chain packing will facilitate the preparation of novel nanostructures and applications in advanced materials.

In the present work, we performed a dissipative particle dynamics simulation to study the phase behaviors of SCLC block copolymers, which consists of flexible **A** block and flexible **B** block grafted by rigid **C** side chains. The effects of **A**, **C** block lengths, and graft number on the phase structures were examined. Stability regions of various mesophases were constructed in space of **C** block length and **A** block length (or graft number and **A** block length). The packing ordering of rigid **C** side chains was also studied. Additionally, a comparison of the phase behaviors between SCLC block copolymers and flexible copolymers was made. The simulation results were also compared with the available experimental observations.

## 2.   METHOD AND MODEL

### 2.1   Simulation Method

Dissipative particle dynamics was first proposed by Hoogerbrugge and Koelman,[44,45] which is suitable for complex fluids.[46-48] It is a combination of molecular dynamics, lattice-gas automata, and Langevin dynamics, which obeys Galilean invariance, isotropy, mass conservation, and momentum conservation. In the method, a bead having mass $m$ represents a block or cluster of atoms or molecules moving together in a coherent fashion. The DPD beads are subject to soft potentials and governed by predefined collision rules.[49]

In the method, the force $\mathbf{f}_i$ acting on bead $i$ is a pairwise additive force, consisting of the conservative force ($\mathbf{F}_{ij}^{C}$), dissipative force ($\mathbf{F}_{ij}^{D}$), and random force ($\mathbf{F}_{ij}^{R}$), given by[48]

$$\mathbf{f}_i = \sum_{j \neq i}(\mathbf{F}_{ij}^{C} + \mathbf{F}_{ij}^{D} + \mathbf{F}_{ij}^{R}) \tag{1}$$

The conservative force is a soft repulsion taking the form as follows:

$$\mathbf{F}_{ij}^{C} = a_{ij}\sqrt{\omega(r_{ij})}\hat{\mathbf{r}}_{ij} \tag{2}$$

where $a_{ij}$ is the maximum repulsive interaction between beads $i$ and $j$, $\mathbf{r}_{ij} = \mathbf{r}_i - \mathbf{r}_j$, $r_{ij} = |\mathbf{r}_{ij}|$, $\hat{\mathbf{r}}_{ij} = \mathbf{r}_{ij}/r_{ij}$, and $\omega(r_{ij})$ is the weight function given by

$$\omega(r_{ij}) = \begin{cases} (1 - r_{ij}/r_c)^2 & (r_{ij} < r_c) \\ 0 & (r_{ij} \geq r_c) \end{cases} \tag{3}$$

according to the study by Groot and Warren, and $r_c$ is the cutoff radius ($r_c = 1.0$). The dissipative force is a friction force that acts on the relative velocities of beads, defined by

$$\mathbf{F}_{ij}^{D} = -\gamma \omega^{D}(r_{ij})(\hat{\mathbf{r}}_{ij} \cdot \mathbf{v}_{ij})\hat{\mathbf{r}}_{ij} \tag{4}$$

and the random force, compensating the loss of kinetic energy due to the dissipative force, is defined by

$$\mathbf{F}_{ij}^{R} = \sigma \omega^{R}(r_{ij})\theta_{ij}\hat{\mathbf{r}}_{ij} \tag{5}$$

where $\mathbf{v}_{ij} = \mathbf{v}_i - \mathbf{v}_j$, $\gamma$ is the friction coefficient, $\sigma$ is the noise amplitude, $\omega^{D}(r_{ij})$ and $\omega^{R}(r_{ij})$ are weight functions vanishing for $r > r_c$ that describe the range of the dissipative and random forces, and $\theta_{ij}$ is a randomly fluctuating variable with Gaussian statistics:

$$\langle \theta_{ij}(t) \rangle = 0, \quad \langle \theta_{ij}(t)\theta_{kl}(t') \rangle = (\delta_{ik}\delta_{jl} + \delta_{il}\delta_{jk})\delta(t - t'). \tag{6}$$

In order to satisfy the fluctuation-dissipation theorem and for the system to evolve to an equilibrium state that corresponds to the Gibbs canonical ensemble, only one of $\omega^{D}(r_{ij})$ and $\omega^{R}(r_{ij})$ can be chosen arbitrarily and the other one is then fixed by the relation[47,48]

$$\omega^{D}(r_{ij}) = \left[\omega^{R}(r_{ij})\right]^2 = \omega(r_{ij}) \tag{7}$$

And the values of parameters $\gamma$ and $\sigma$ are coupled by

$$\sigma^2 = 2\gamma k_{B}T \tag{8}$$

where $T$ is the absolute temperature, and $k_B$ is the Boltzmann constant.

For the copolymers, the interaction force between bonded beads is considered as harmonic spring force,

$$\mathbf{F}_{ij}^{S} = C(1 - r_{ij} / r_{eq})\hat{\mathbf{r}}_{ij} \tag{9}$$

where $C$ is the spring constant and $r_{eq}$ is the equilibrium bond distance. In order to reinforce the rigidity of the side chains, one angle force is added between every two consecutive bonds. The bond angle $\theta$ is constrained as 180°, and the angle force is defined by

$$\mathbf{F}^{A} = -\nabla[k_{\theta}(\theta - \pi)^{2}] \tag{10}$$

where $k_{\theta}$ is the angle constant. The larger the $k_{\theta}$ value, the more rigid the side chains.

In the DPD method, reduced units are adopted for all physical quantities.[48] The units of mass, length, time, and energy are defined by $m$, $r_{c}$, $\tau$, and $k_{B}T$, respectively. The time unit $\tau$ can be formulated by

$$\tau = \sqrt{(mr_{c}^{2})/k_{B}T} \tag{11}$$

and its real value can be estimated by matching the simulated lateral diffusion coefficient to the experimental measured value.

## 2.2 Model and Condition

In the simulation, we constructed a coarse-grained model of SCLC block copolymers, as typically shown in Figure 1. The copolymer consists of a flexible **A** block with $x$ beads and a flexible **B** block with $y$ beads that is grafted by $n$ rigid **C** chains with $z$ beads on each chain. The block copolymers are denoted by the type of $\mathbf{A}_{x}$-$b$-$(\mathbf{B}_{y}$-$g$-$n\mathbf{C}_{z})$, where $b$ and $g$ are short for "block" and "graft", respectively. In the expression, $y = 2n$, therefore, the total bead number $N$ in one copolymer molecule satisfies: $N = x + n(z + 2)$. Note that this model can represent varieties of analogous SCLC copolymers that possess characters of microphase separation and LC ordering, such as the block copolymer containing flexible P4VP block and the rigid side chains of azobenzene moieties.[34,50]

All the simulations were carried on a cubic box (30 × 30 × 30) with periodic boundary conditions adopting NVT ensemble. The temperature $T$ was set to be 1.0 except for the study of

temperature effect. The friction coefficient $\gamma$, noise amplitude $\sigma$, and number density $\rho$ were set to 4.5, 3.0, and 3.0, respectively. The time step was set as $\Delta t = 0.02\tau$. The spring constant $C$ and equilibrium bond distance $r_{eq}$ were chosen as 100 and 0.8. A larger angle constant $k_\theta$ of 200 was set to ensure the rigidity of **C** side chains. The interaction between identical species was set to be 25, while the interaction parameters between different species were all fixed as 60, implying that different species are incompatible. To capture the equilibrated structures, $2.0 \times 10^6$ DPD steps were carried out. When studying the ordered packing of rigid chains, we annealed the system from $T = 1.0$ to $T = 0.1$ during $1.8 \times 10^7$ DPD steps.

## 3. RESULTS AND DISCUSSION

In this work, three-component SCLC block copolymers were applied to form diverse mesophases in melt. The molecular architecture including block length and graft number, and the temperature are important parameters governing the phase behaviors of SCLC copolymers. The lengths of **A**, **B**, and **C** blocks are denoted by the bead numbers of blocks in one polymer chain, *i.e.*, $x = N_A$, $y = N_B$, and $z = N_C$. In what follows, the influences of these parameters, that $N_A$, $N_C$, $n$ and $T$, were particularly examined. The simulation of similar $A_x$-$b$-($B_y$-$g$-$nC_z$) with **C** blocks changing to flexible was additionally carried out, in order to explore the influence of the rigidity of side chains.

### 3.1 Influence of Block Lengths and Graft Number on Phase Behavior

In the subsection, the phase behaviors of SCLC block copolymers as a function of **A** block length $N_A$, **C** block length $N_C$, and graft number $n$ were investigated. The $N_A$ was varied from 4 to 100, while $N_C$ was changed from 5 to 8. And the block copolymers with graft number $n = 2, 3, 4$ and 5 were considered. For various $n$, the **B** block length $N_B$ should be chosen according to the relation $y = 2n$. All phase structures were equilibrated at temperature $T = 1.0$, corresponding to a melt state.

We first considered the model of SCLC block copolymer with $N_B = 8$, $N_C = 6$, and $n = 4$. Figure 2 shows the self-assembly structures observed at various lengths $N_A$ of **A** blocks. As can be seen from Figure 2a, the SCLC block copolymers form a spherical structure (**S$_A$**) when **A** block length is smaller ($N_A = 4$). The **A** spheres surrounded by **B** blocks are dispersed in a matrix of **C** blocks. When $N_A$ increases into 8, the block copolymers phase-separate into a cylindrical structure (**C$_A$**) where the cylinders of **A** blocks covered by **B** blocks are hexagonally aligned in the matrix of **C** blocks (Figure 2b). As $N_A$ is 24, a gyroid phase (**G$_A$**) with the minority domains of **B**-covered **A** blocks and continuous matrix of **C** blocks is observed (see Figure 2c). With further increasing $N_A$, a lamellar structure (**L**) is produced at $N_A = 48$, which contains one thick **A** lamella and three thin **BCB** lamellae, as shown in Figure 2d. Figure 2e shows a gyroid structure (**G$_C$**) with the **B**-covered **C** blocks forming the minority domains in the **A** matrix at $N_A = 80$. It is apparent from Figure 2 that the ordered phase transition of **S$_A$**→**C$_A$**→**G$_A$**→**L**→**G$_C$** occurs as the $N_A$ increases. The phase transition can be explained as follows. When the **A** blocks is short, the **A** blocks occupy the minor domains, forming phases such as **S$_A$** and **C$_A$**. As the length of **A** blocks increases, the chains become stretched in the minor domains, and the conformation entropy becomes unfavorable. To relax the **A** blocks, **L** and **G$_C$** are formed. In these structures, the **A** blocks occupy the major domains. Through the phase transitions, the conformation entropy arising from chain stretching becomes favorable. However, the interfacial/surface energy increases.

Subsequently the effect of **C** block length $N_C$ was examined. Combining the effects of $N_A$ and $N_C$, the thermodynamic stability regions of phase-separated structures were constructed. Figure 3 presents the phase stability regions in space of $N_C$ vs $N_A$ for SCLC block copolymers with $N_B = 8$ and $n = 4$. The mesophases include **S$_A$**, **C$_A$**, **G$_A$**, **L**, and **G$_C$**. It can be found that with increasing $N_C$, the **C$_A$** and **L** regions become narrower and wider, respectively, while the width of **G$_A$** region keeps

unchanged roughly. Note that when the $N_C$ increases to 7, the **$S_A$** phase disappears, and the **$C_A$** phase

also disappears as $N_C$ is 8. The spherical and cylindrical structures are unfavorable to form for longer

**C** side chains. The boundaries of **$C_A$** and **L** regions tend to shift toward smaller $N_A$, while the left

and right boundaries of **$G_A$** region respectively move to smaller $N_A$ and larger $N_A$. It suggests that at

a constant $N_A$ the lamellae are easier to form than spheres, cylinders, and gyroid for longer **C** blocks.

In Figure 3, the lamellar phase occupies wider region at larger $N_C$. With increasing $N_C$, the

stretching action of **A** blocks decreases while the orientation of **C** blocks takes over the greater

function. To maintain the system stability, the lamellar structure is a preferable structure and the

lamellar region is broadened at higher $N_C$. At higher $N_A$, the phase transition of **$G_C$→L** appears as

$N_C$ increases. As the rigid **C** blocks become long, the blocks become orientations to reduce the loss

of orientation entropy. Thus, In **L** phases, the rigid **C** blocks can be packed entropically favorable

compared with **$G_C$** phases. On the other hand, the interfacial/surface energy becomes

unfavorable.[53,54] On the other hand, at constant $N_C$, as the $N_A$ increases, the phase transition

experiences the progress of **$S_A$→$C_A$→$G_A$→L→$G_C$**. Originally, the volume fraction of **A** blocks is

too low, so that **C** blocks incline to form the matrix and the **$S_A$**, **$C_A$** and **$G_A$** are formed. When $N_A$ is

large enough, the lamellar phase was generated with interaction of **A** blocks and **C** blocks. Further

increasing the $N_A$ value, the volume fraction of LC component is low, so that the orientation of **C**

block has only a slight effect. Therefore, the **L** phase is transformed into the **$G_C$** phase.

In addition to the block length, the effect of the graft number *n* on the phase behavior was also

studied. The phase stability regions in space of *n* vs $N_A$ are shown in Figure 4 where the **C** block

length $N_C$ is set to be 6. At *n* = 2 and 3, no **$S_A$** and **$C_A$** phases are formed. As the *n* increases, the **$C_A$**,

**$G_A$**, and **L** regions become wider. The boundaries of **$C_A$**, **$G_A$**, and **L** regions all move to larger $N_A$,

which is different from the effect of $N_C$. The SCLC block copolymers tend to form the **$G_C$** phase for

lower $n$ but form the **L** or $\mathbf{G_A}$ phase for higher $n$ at a constant $N_A$. It is discovered from Figure 4 that the graft number $n$ markedly influences the phase structures of SCLC block copolymers. As the graft number increases, the volume fraction of LC component increases, while the volume fraction of **A** blocks decreases. Similar to the discussion above, the increasing of LC component is favorable for packing ordering, resulting in that the lamellar phase occupies wider region at larger $n$. Overall, the formation of different phase structures can be speculated as a balance of stretching and orientation from **A** blocks and **C** blocks separately.

### 3.2   Influence of Temperature on Packing Ordering of Rigid C Side Chains

In this subsection, the packing ordering of rigid **C** side chains in various ordered structures was investigated. The orientation degree was characterized by order parameter $S$, which is an average value of order parameter $S_i$ of $i$-th rigid chain. The $S_i$ is defined by $S_i = \dfrac{3(\mathbf{u}_i \cdot \mathbf{u}_d)^2 - 1}{2}$, where $\mathbf{u}_i$ is the normalized vector of $i$-th rigid chain, $\mathbf{u}_d$ is the normalized vector of orientation direction, which is determined by iteration to find the maximum value of $S_i$ by dividing the polar-coordinate space into pieces. First, we studied the effect of temperature on the chain packing state in several typical structures through annealing the systems from a higher temperature ($T = 1.0$) to a lower temperature ($T = 0.1$). Then we calculated the order parameter $S$ as a function of temperature at various $N_A$ and $N_C$.

Three typical structures, $i.e.$, $\mathbf{C_A}$, **L**, and $\mathbf{G_C}$ phases, were taken for example. When the temperature was cooled to 0.1, the structures formed by SCLC block copolymers at various $N_A$ are presented in Figure 5. We mainly focused on the packing of rigid **C** side chains. As shown in Figure 5a, a cylindrical structure ($\mathbf{C_A}$) is formed at $N_A = 8$, where the **C** chains are packing orderly and perpendicularly to the long axes of cylinders consisting of **A** blocks covered by **B** blocks. Figure 5b shows a lamellar structure with the **C** chains parallel with each other at $N_A = 56$. The highly

orientational packing of rigid chains was achieved at lower temperature, and the lamellar structure is a smectic-like structure. At $N_A = 80$, the gyroid structure (**G$_C$**) with **B**-covered **C** blocks forming the minority domains in the **A** matrix indicates that the rigid **C** chains are aligned with each other in a twisting manner, as shown in Figure 5c. It is concluded from Figure 5 that rigid chains can be packing more regularly when decreasing the temperature to a lower value.

In order to further understand the influence of temperature on the packing ordering of rigid **C** chains, the order parameters of **C** chains in a lamellar structure were explored at various temperatures. The results at $N_A = 48$ are shown in Figure 6. The insert shows the typical simulation snapshots at various temperatures. At $T = 1.0$, the order parameter $S$ is low, where an unordered lamella was obtained. As the temperature decreases, the $S$ increases gradually, and finally achieves a plateau. The $S$ is about 0.75 when $T$ decreases to 0.2, indicating that the rigid chains are orientated and packed regularly in the lamellar domains. A smectic-like structure is formed gradually with decreasing the system temperature. The result implies that the temperature has marked influences on the packing ordering of rigid chains.[55,56]

Subsequently, to study the effect of lengths of **A** and **C** blocks on chain packing ordering, the $S$ values of **C** side chains as a function of temperature at various $N_C$ and $N_A$ were calculated, where only the lamellar phase was considered. Figure 7a shows the order parameter $S$ at the temperature ranging from 1.0 to 0.1 for block copolymers with $N_C = 5, 6, 7,$ and 8. The other parameters are $N_A = 56$, $N_B = 8$, and $n = 4$. As can be seen, for any $N_C$ the $S$ exhibits the same trend that it increases with decreasing the temperature. At a fixed temperature, the effect of $N_C$ can be viewed. The $S$ has a higher value at larger $N_C$, indicating that longer **C** chains can benefit their ordered packing. On the other hand, the $S$ values *versus* temperature at various $N_A$ were presented in Figure 7b. The $N_A$ was varied from 40 to 64, while $N_B$, $N_C$, and $n$ were fixed as 8, 6, and 4, respectively. It shows that at

various $N_A$, the $S$ has the similar trend with the elevation of temperature (discussed above). However,

the $N_A$ was discovered to have a slight influence on the $S$ values. From Figure 7, we can find that the

length of rigid **C** side chains is crucial to chain packing ordering relative to the length of flexible **A**

chains, and the **A** block length mainly influences the phase regions.


### 3.3   Comparison with Flexible Copolymers and Available Experimental Observations

In this subsection, we made a comparison between the phase behaviors of flexible block

copolymers and SCLC block copolymers. As can be seen in Figure 8a, the flexible block copolymer

possesses the same molecular structure only with the side chain transiting from rigidity into coil. The

block component and interaction parameters of flexible copolymers were chosen the same as the

SCLC copolymers. This can benefit knowing the effect of introduction of rigid side chains on the

phase behaviors of three-component block copolymers. Through adjusting the lengths of **C** and **A**

blocks, the phase stability regions in space of $N_C$ and $N_A$ were also constructed. Then we compared

the simulation results of SCLC copolymers and available experimental observations.

Figure 8b shows the phase stability regions in space of $N_C$ vs $N_A$ for flexible block copolymers

with $N_B = 8$ and $n = 4$ at $T = 1.0$. The $N_A$ was varied from 4 to 80, while $N_C$ was changed from 5 to 8.

Similar to SCLC block copolymers, $\mathbf{S_A}$, $\mathbf{G_A}$, **L**, and $\mathbf{G_C}$ regions were obtained. However, under the

parameter conditions employed, cylindrical structures cannot be observed, and the $\mathbf{C_A}$ region is

lacked. Relative to the SCLC block copolymers, we can also find that the $\mathbf{G_A}$ region becomes

broader while the **L** region is narrower for flexible block copolymers. The lamellar structures are

generated at larger $N_A$, and the boundary between the $\mathbf{G_A}$ and **L** regions moves to larger $N_A$. It

suggests that the introduction of rigid side chains is favorable to the formation of lamellar structures

at smaller $N_A$. Besides the diversity in the phase boundaries, the ordering of chain packing is also

different for flexible and SCLC copolymers. In flexible copolymers, the chains are unable to orient as rigid blocks and thereby parked irregularly. In the microphase separation, the flexible chains are stretched to accommodate the structures, while the rigid blocks change their orientations to adjust the structures.

Recently, some experimental observations regarding the SCLC copolymers are available in the literatures for supporting our predictions.[50-52,57] Mao *et al*. synthesized a series of SCLC block copolymers by attaching azobenzene mesogenic groups to the isoprene block of polystyrene-*b*-poly(1,2-&-3,4-isoprene) (PS-*b*-PI) block copolymers *via* acid chloride coupling.[50] The bulk structures of the SCLC block copolymers were studied and found to be controlled by the volume fraction of LC component. The formed coil cylinders at higher LC volume fraction are transformed into a lamellar structure and then into a bicontinuous structure with the minority domains of LC component as the LC volume fraction decreases. Anthamatten and coworkers also found that the SCLC block copolymers of polystyrene and methacrylates containing (*s*)-2-methyl-1-butyl-4'-(((4-hydroxyphenyl)carbonyl)oxy)-1,1'-biphenyl-4-carboxylate mesogens (PS-*b*-HBPB) can form hexagonally close-packed PS cylinders at higher LC volume fraction, while they self-assemble into completely lamellar structures or predominately lamellar structures at lower LC volume fraction.[51,52] These experimental observations are in qualitative accordance with the simulated phase transition from $C_A$ to $L$ and then to $G_C$ with increasing $N_A$.

M. Yamada and coworkers prepared a kind of SCLC copolymer containing polystyrene segment and 6-[4-(4-methoxyphenyl)phenoxy]-hexyl methacrylate (MPPHM) segment,[57] which is similar with our model as the MPPHM segment can be divided into **B** block and **C** block. These copolymers exhibited the well-defined lamellar type of segregation, and the side chain LC segments formed crystal, smectic A, and isotropic arrangements with increasing temperature. This tendency coincides

well with our finding that the order parameter increases with decreasing the temperature (see Figures

6 and 7). In contrast with the similarity, some difference is also observed. For example, in our

simulations, the $G_A$ structure with the coil blocks forming the minority domains was predicted, but it

was not found in the experiments. The difference may be resulted from the coarse-grained model in

the DPD simulations and the limited samples in the experiments. In addition, our predictions also

reveal the mechanism of phase transition, which may provide guidance for further studies of phase

structures of SCLC block copolymers.

In this work, the phase behaviors of SCLC block copolymers were investigated by DPD method

for the first time. Various ordered nanostructures were formed including hexagonally packed

cylinders seldom observed in existing researches, and the morphological window of this category of

copolymers was further expanded. The architecture parameters of SCLC copolymers including the

block length and graft number were found to play important roles in determining the phase structures.

In addition, the simulations provide chain packing information which cannot be captured in

experiments. The simulation results could be helpful for developing promising strategies to control

the complex structures formed by SCLC copolymers.


## 4. CONCLUSIONS

In this work, we have investigated the phase behavior of the SCLC block copolymers by the

DPD simulations. It was found that the $S_A$, $C_A$, $G_A$, $L$, and $G_C$ phases are formed sequentially as the

$N_A$ increases. Moreover, with increasing the value of $N_C$ or $n$, the lamella phases with extensive

region were formed. The thermodynamic stability regions of these phases were constructed by

combining these two effects, i.e., $N_C$ vs. $N_A$ and $n$ vs. $N_A$. The phase transitions are the balance of

interaction enthalpy and the entropy resulted from the stretching of flexible **A/B** chains and the

orientation of rigid **C** chains. On cooling the temperature, the order parameters of **C** blocks increase and the packing of rigid **C** side chains exhibit higher ordering. Compared with flexible copolymers, the regions of **L** phases enlarge and the boundary between the **G$_A$** and **L** regions moves to lower $N_A$ for the SCLC copolymers. In addition, a general agreement with experimental observations was found, but with some difference. The difference may be resulted from the coarse-grained model in DPD simulations and the limited samples in experiments. The present work could be of guiding significance for understanding the phase behavior of SCLC block copolymers.

16

## REFERENCES

[1]  R. Resendes, J. A. Massey, H. Dorn, K. N. Power, M. A. Winnik and I. Manners, *Angew. Chem. Int. Ed.*, 1999, **38**, 2570-2573.

[2]  W. van Zoelena and G. ten Brinke, *Soft Matter*, 2009, **5**, 1568-1582.

[3]  Z. Li, E. Kesselman, Y. Talmon, M. A. Hillmyer and T. P. Lodge, *Science*, 2004, **306**, 98-101.

[4]  D.-G. Kim, H. Kang, S. Han, H. J. Kima and J.-C. Lee, *RSC Adv.*, 2013, **3**, 18071-18081.

[5]  H. Otsukaa, Y. Nagasakib and K. Kataoka, *Curr. Opin. Colloid Interface Sci.*, 2001, **6**, 3-10.

[6]  Z. Wang, G. Wen, F. Zhao, C. Huang, X. Wang, T. Shi and H. Li, *RSC Adv.*, 2014, **4**, 29595-29603.

[7]  V. Percec, C. H. Ahn and G. Ungar, *Nature*, 1998, **391**, 161-164.

[8]  S. B. Darling, *Prog. Polym. Sci.*, 2007, **32**, 1152-1204.

[9]  M. W. Matsen and F. S. Bates, *Macromolecules*, 1996, **29**, 7641-7644.

[10] J. Chatterjee, S. Jain and F. S. Bates, *Macromolecules*, 2007, **40**, 2882-2896.

[11] R. Nagarajan and K. Ganesh, *J. Chem. Phys.*, 1989, **90**, 5843-5856.

[12] S. A. Jenekhe and X. L. Chen, *Science*, 1999, **283**, 372-375.

[13] S. A. Jenekhe and X. L. Chen, *Science*, 1998, **279**, 1903-1907.

[14] T. Kato, *Science*, 2002, **295**, 2414-2418.

[15] S.-C. Tsao and C.-T. Lo, *RSC Adv.*, 2014, **4**, 23585-23594.

[16] J.-G. Lia and S.-W. Kuo, *RSC Adv.*, 2011, **1**, 1822-1833.

[17] W. Sun, X. He, X. Liao, S. Lin, W. Huang and M. Xie, *J. Appl. Polym. Sci.*, 2013, **130**, 2165-2175.

[18] P. Fatás, J. Bachl, S. Oehm, A. I. Jiménez1, C. Cativiela and D. D. Díaz, *Chem. Eur. J.*, 2013, **19**, 8861-8874.

[19] K. Gayathrt, S. Balamurugan and P. Kannan, *J. Chem. Sci.*, 2011, **123**, 255-263.

[20] O. Ikkala and G. ten Brinke, *Chem. Commun.*, 2004, 2131-2137.

[21] G. ten Brinke and O. Ikkala, *Chem. Rec.*, 2004, **4**, 219-230.

[22] H. Fischer and S. Poser, *Acta Polym.*, 1996, **47**, 413-428.

[23] R. P. Nieuwhof, A. T. M. Marcelis, E. J. R. Sudholter, S. J. Picken and W. H. de Jeu, *Macromolecules*, 1999, **32**, 1398-1406.

[24] A. Laiho, P. Hiekkataipale, J. Ruokolainen and O. Ikkala, *Macromol. Chem. Phys.*, 2009, **210**, 1218-1223.

[25] A. J. Soininen, I. Tanionou, N. ten Brummelhuis, H. Schlaad, N. Hadjichristidis, O. Ikkala, J. Raula, R. Mezzenga and J. Ruokolainen, *Macromolecules*, 2012, **45**, 7091-7097.

[26] J. de Wit, G. A. van Ekenstein, E. Polushkin, K. Kvashnina, W. Bras, O. Ikkala and G. ten Brinke, *Macromolecules*, 2008, **41**, 4200-4204.

[27] S. Lin, Y. Wang, C. Cai, Y. Xing, J. Lin, T. Cheng and X. He, *Nanotechnology*, 2013, **24**, 085602.

[28] Y. Wang, S. Lin, M. Zang, Y. Xing, X. He, J. Lin and T. Chen, *Soft Matter*, 2012, **8**, 3131-3138.

[29] A. Martínez-Felipe, C. T. Imrie and A. Ribes-Greus, *Ind. Eng. Chem. Res.*, 2013, **52**, 8714-8721.

[30] E. Barmatov, *Macromolecules*, 2002, **35**, 3076-3082.

[31] A. Kozak, J. J. Moura-Ramos, G. P. Simon and G. Williams, *Macromol. Chem. Phys.*, 1989, **190**, 2463-2476.

[32] S. Chen, A. Ling and H.-L. Zhang, *J. Polym. Sci., Part A: Polym. Chem.*, 2013, **51**, 2759-2768.

[33] S. H. Goh, Y. H. Lai and S. X. Cheng, *Liq. Cryst.*, 2001, **28**, 1527-1538.

[34] J. T. Korhonen, T. Verho, P. Rannou and O. Ikkala, *Macromolecules*, 2010, **43**, 1507-1514.

[35] L. Wang, J. Lin and L. Zhang, *Langmuir*, 2009, **25**, 4735-4742.

[36] L. Wang, T. Jiang and J. Lin, *RSC Adv.*, 2013, **3**, 19481-19491.

[37] M. Kenward and M. D. Whitmore, *J. Chem. Phys.*, 2002, **116**, 3455-3470.

[38] M. Mondeshki, G. Mihov, R. Graf, H. W. Spiess and K. Müllen, *Macromolecules*, 2006, **39**, 9605-9613.

[39] T. Jiang, L. Wang and J. Lin, *RSC Adv.*, 2014, **4**, 35272–35283.

[40] T. Jiang, L. Wang, S. Lin, J. Lin and Y. Li, *Langmuir*, 2011, **27**, 6440-6448.

[41] M. Shah, V. Pryamitsyn and V. Ganesan, *Macromolecules*, 2008, **41**, 218-229.

[42] M. Anthamatten and P. T. Hammond, *J. Polym. Sci., Part B: Polym. Phys.*, 2001, **39**, 2671-2691.

[43] L. M. Stimson and M. R. Wilson, *J. Chem. Phys.*, 2005, **123**, 034908.

[44] P. J. Hoogerbrugge and J. M. V. A. Koelman, *Europhys. Lett.*, 1992, **19**, 155-160.

[45] J. M. V. A. Koelman and P. J. Hoogerbrugge, *Europhys. Lett.*, 1993, **21**, 363-368.

[46] Y. Xu, J. Feng and H. Liu, *Mol. Simul.*, 2008, **34**, 559-565.

[47] P. Espanol and P. B. Warren, *Europhys. Lett.*, 1995, **30**, 191-196.

[48] R. D. Groot and P. B. Warren, *J. Chem. Phys.*, 1997, **107**, 4423-4435.

[49] Y.-J. Sheng, C.-H. Nung and H.-K. Tsao, *J. Phys. Chem. B*, 2006, **110**, 21643-21650.

[50] G. Mao, J. Wang, S. R. Clingman and C. K. Ober, *Macromolecules*, 1997, **30**, 2556-2567.

[51] M. Anthamatten and P. T. Hammond, *Macromolecules*, 1999, **32**, 8066-8076.

[52] W. Y. Zheng and P. T. Hammond, *Macromolecules*, 1998, **31**, 711-721.

[53] K. Gordon, B. Sannigrahi, P. Mcgeady, X. Q. Wang, J. Mendenhall and I. M. Khan, *J. Biomater. Sci., Polym. Ed.*, 2009, **20**, 2055-2072.

[54] S. T. Milner, *Science*, 1991, **251**, 905-914.

[55] A. AlSunaidi, W. K. den Otter and J. H. R. Clarke, *Phil. Trans. R. Soc. Lond. A*, 2004, **362**, 1773-1781.

[56] A. AlSunaidi, W. K. den Otter and J. H. R. Clarke, *J. Chem. Phys.*, 2009, **130**, 124910.

[57] M. Yamada, T. Iguchi, A. Hirao, S. Nakahama and J. Watanabe, *Polym. J.*, 1998, **30**, 23-30.

**FIGURE CAPTION**

**Figure 1.** Coarse-grained model for the SCLC block copolymers. The beads colored by red, green, and blue represent flexible **A** block, flexible **B** block, and rigid **C** side chains, respectively.

**Figure 2.** Simulated structures formed by SCLC block copolymers with $N_B = 8$, $N_C = 6$, and $n = 4$: (a) spheres, $S_A$, (b) cylinders, $C_A$, (c) gyroid, $G_A$, (d) lamellae, **L**, and (e) gyroid, $G_C$. The subscripts **A** and **C** in **S**, **C**, and **G** denote that the minority domains of ordered structure are formed by **A** and **C** blocks, respectively. From (a) to (e), the lengths $N_A$ of **A** blocks are 4, 8, 24, 48, and 80, respectively. The red, green, and blue colors are assigned to **A**, **B**, and **C** blocks, respectively.

**Figure 3.** Phase stability regions of SCLC block copolymers in space of $N_C$ vs $N_A$. The ordered regions are denoted as **S** (spheres), **C** (hexagonally packed cylinders), **G** (bicontinuous gyroid), and **L** (lamella). The subscripts **A** and **C** in **S**, **C**, and **G** indicate that the minority domains of ordered structure are formed by **A** and **C** blocks, respectively. The **B** block length $N_B$ is fixed as 8, and the graft number $n$ is 4. Regions of $S_A$ (◯), $C_A$ (△), $G_A$ (▢), **L** (◇), and $G_C$ (⬠) phases are shown.

**Figure 4.** Phase stability regions in space of $n$ vs $N_A$ for SCLC block copolymers with $N_C = 6$. Regions of $S_A$ (◯), $C_A$ (△), $G_A$ (▢), **L** (◇), and $G_C$ (⬠) phases are shown.

**Figure 5.** Typical structures formed by SCLC block copolymers at various $N_A$ when the temperature was cooled to 0.1: (a) cylindrical structure ($C_A$) at $N_A = 8$, (b) lamellar structure (**L**) at $N_A = 56$, and

(c) gyroid structure ($G_C$) at $N_A = 80$. In Figure (c), the local packing of **C** side chains is also shown.

**Figure 6.** Order parameter $S$ of rigid **C** side chains in a lamellar structure as a function of the system temperature $T$. The lamellae are formed by block copolymers with $N_A = 48$, $N_B = 8$, $N_C = 6$, and $n = 4$. The inset shows the typical simulation snapshots at various $T$.

**Figure 7.** Order parameters $S$ of **C** chains as a function of temperature for SCLC block copolymers (a) with various $N_C$, (b) with various $N_A$. In figure a, the $N_C$ was changed from 5 to 8, and the other parameters are $N_A = 56$, $N_B = 8$, and $n = 4$. In figure b, the $N_A$ was varied from 40 to 64, while $N_B$, $N_C$, and $n$ were fixed as 8, 6, and 4, respectively.

**Figure 8.** (a) The similar flexible block copolymer with SCLC copolymer except the coil side chain. (b) Phase stability regions of flexible block copolymers in space of $N_C$ vs $N_A$ at $T = 1.0$. The regions of $S_A$, $G_A$, **L**, and $G_C$ phases are obtained. The **B** block length $N_B$ is fixed as 8, and the graft number $n$ is 4.
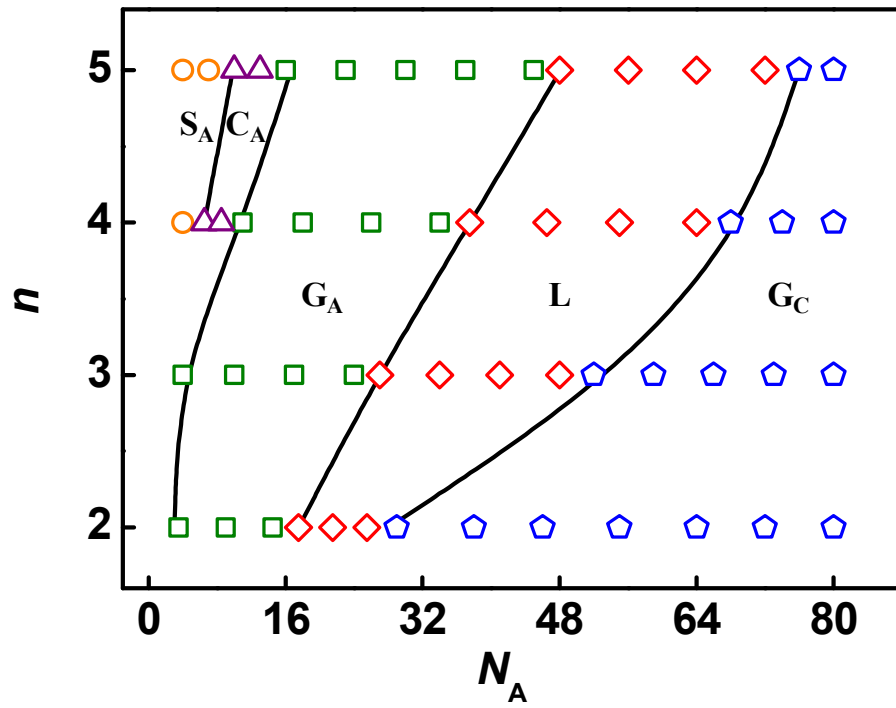
**FIGURES**
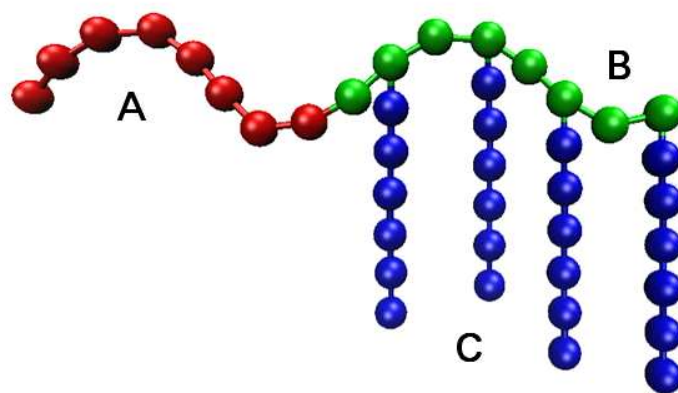


**Figure 1.**
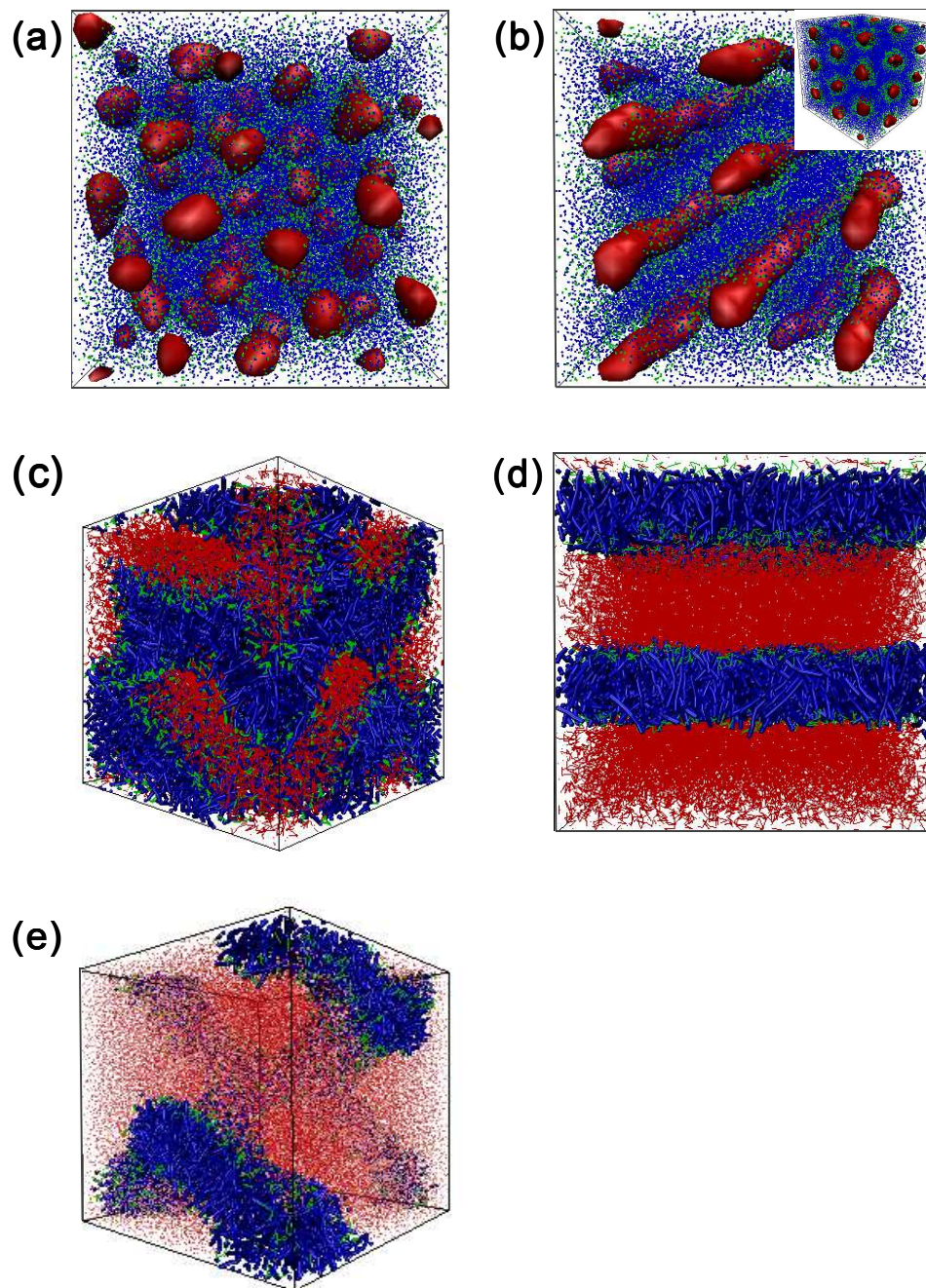
**Figure 2.**
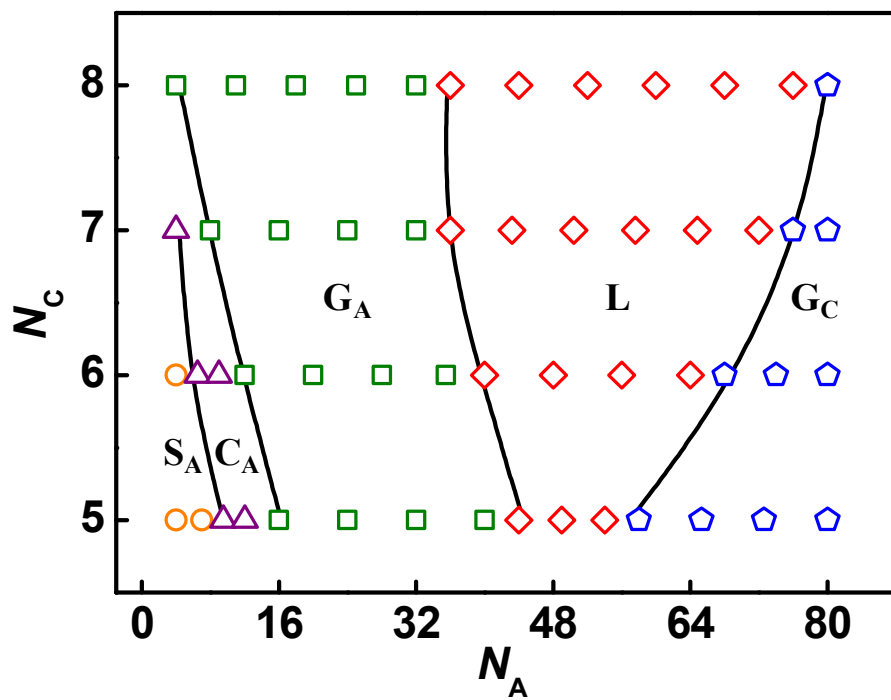
**Figure 3.**

**Figure 4.**
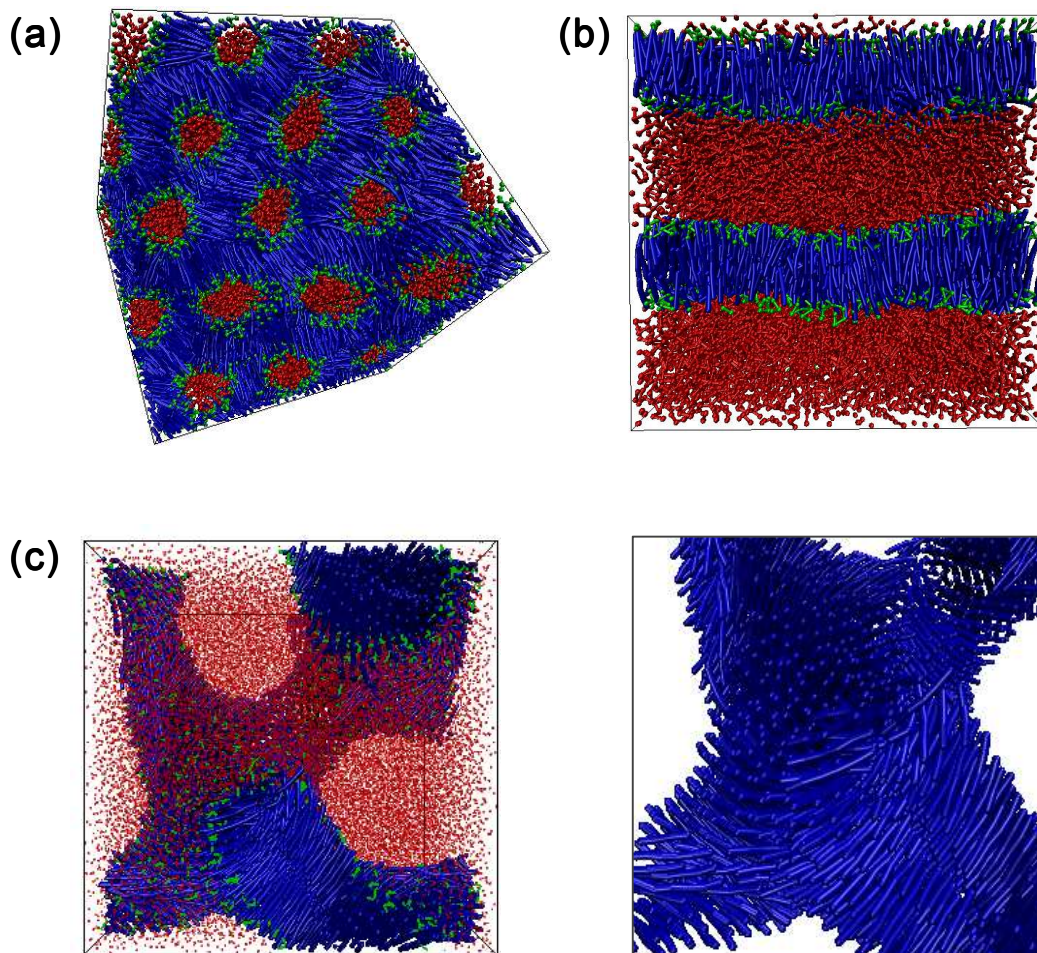
**Figure 5.**
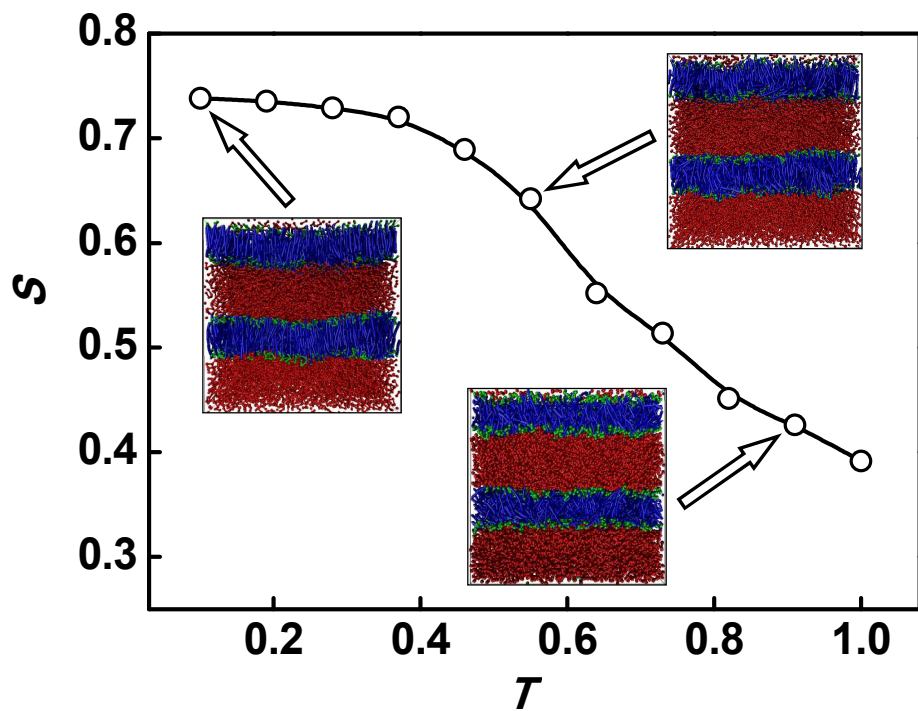
**Figure 6.**
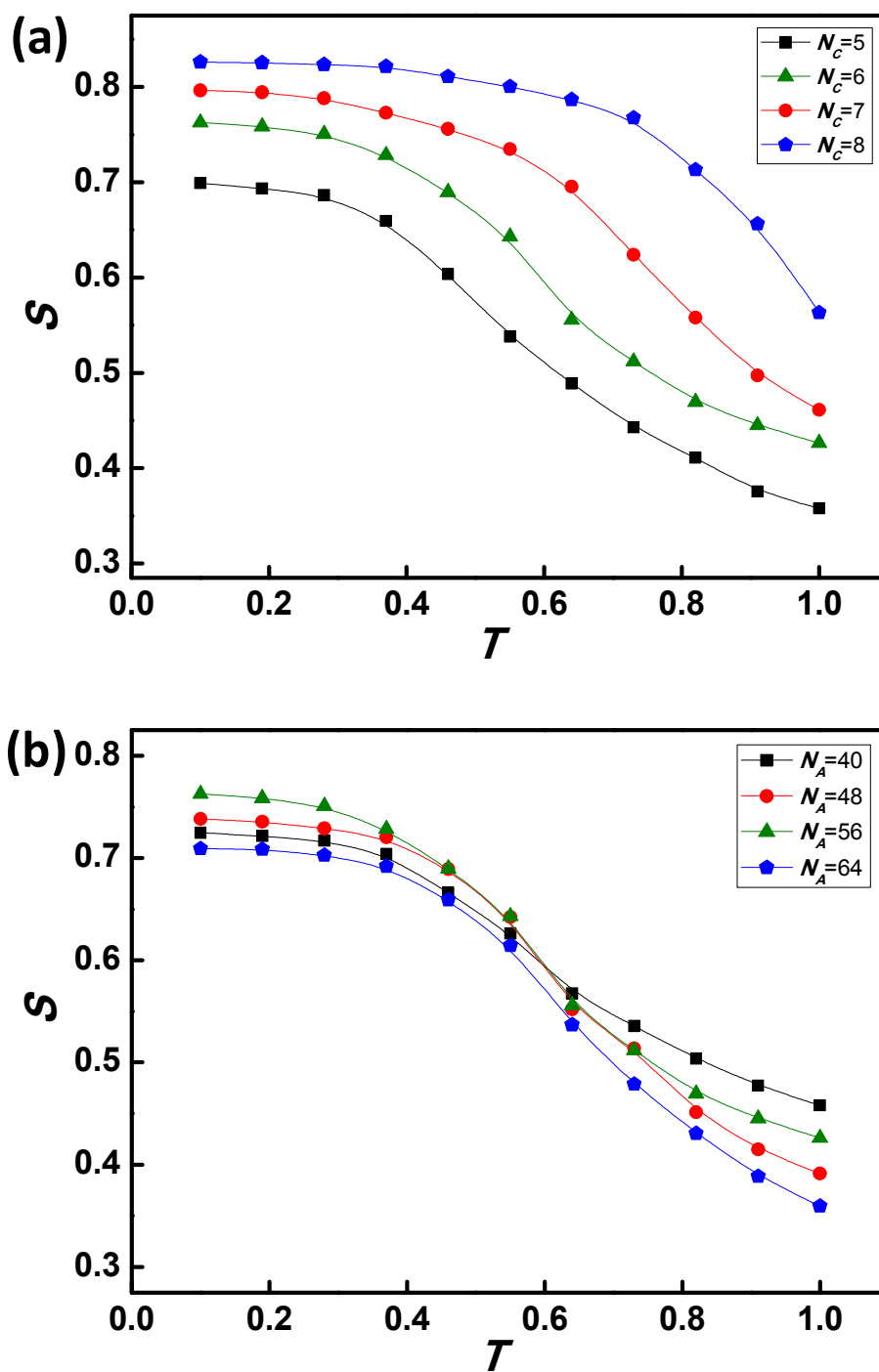
**Figure 7.**

**Figure 8.**

**TOC Image**